Structure and Properties of Lightly Crosslinked Polyvinylidene Fluoride Crystallized from the Deformed Molten State (Special Issue on Polymer Chemistry, XIV)

AUTHOR(S):

Hyon, Suong-Hyu; Kitamaru, Ryozo

Bull. Inst. Chem. Res., Kyoto Univ., Vol. 57, No. 2, 1979

Structure and Properties of Lightly Crosslinked Polyvinylidene Fluoride Crystallized from the Deformed Molten State

Suong-Hyu HYON and Ryozo KITAMARU

Received March 14, 1978

Effects of the deformation upon the supermolecular structure and thermal properties of lightly crosslinked polyvinylidene fluoride are investigated by X-ray diffraction and calorimetric technique. It is confirmed that the molecular chain conformation in drawn samples depends markedly on the draw temperature and draw ratio, and that the long period revealed by low angular X-ray scattering and the scattering intensity increase with increasing draw ratio, when uniaxially streched in the molten state. On the contrary, when samples are uniaxially stretched at a high temperature below the melting point, the long period and scattering intensity decrease with increasing draw ratio. Furthermore, when compressed uniaxially in the molten state, a special planar orientation of the crystal planes of the orthorhombic form of this polymer appears, while no appreciable amount of the β-form appears. The (200) crystal plane is preferentially oriented parallel to the film surface for samples made in such a mode, but when compressed or biaxially stretched in the partially crystallized state, other planar orientations such as (010) and (110) are produced without the (200) orientation.

KEY WORDS: Polyvinylidene fluoride / Crystal transformation / Planar orientation /

INTRODUCTION

The polyvinylidene fluoride (hereafter, abbreviated as PVDF) is known as having a characteristic electric property and widely used as piezoelectric films. It has good physico-mechanical properties as well as excellent resistance to chemical agents and radiation. Depending on conditions for the polymerization[1], crystallization[2], and thermomechanical treatment,[3] this polymer indicates different crystalline forms such as α- and β-forms with different molecular conformations[4].

For this polymer two different crystalline forms, α and β are known. For example, Lando *et al.*[3] and Galpelin *et al.*[5] reported the increase of α-form when it was stretched at higher temperatures, although the β-form could not be removed perfectly. As can be known by their work, the both crystalline forms of this polymer can be obtained comparatively easily according to the oriented conditions.

As described in previous papers, very characteristic structure and properties appear for linear polyethylene[6-11] and isotactic polypropylene,[12,13] if these polymers are crystallized from the molten state under high degrees of molecular orientation, using irradiation crosslinking. This paper deals with a similar attempt for polyvinylidene fluoride.

* 玄 丞烋, 北丸竜三 : Laboratory of Fiber Chemistry, Institute for Chemical Research, Kyoto University, Uji, Kyoto.

EXPERIMENTAL

Sample Preparation

The starting material used in this work was a commercial grade Kynar 400 polymer of Pennsalt Chemical Corporation. Viscosity measurements were made in N-N-dimethylacetamide at 25°C, and the viscosity average molecular weight was calculated using the relation[15], $[\eta]=1.93\times10^{-4}M^{0.677}$. The density measurement was made at 30°C by a floating method using mixed solvent of bromoform and chloroform. Table I designates the characteristics of the starting material.

Table I. Characterization of Material

Intrinsic Viscosity	$[\eta]=2.0$
Molecular Weight	$\bar{M}_\eta=8.5\times10^5$
Density at 30°C	1.785 g/cm^3
Melting Point (DSC)	165°C
Amount of head-to tail structure (NMR)	*89.8 %

* A reference value cited in (16)

The intermolecular crosslinking of this polymer is easily achieved with the irradiation of high energy radiations in vacuo.[17] A γ-ray from ^{60}Co was used in this work to prepare crosslinked samples. Films about 1 mm thick of the polymer were irradiated to a dose of 10 and 20 Mrads at room temperature in vacuum. The gel fraction (w_g) of thus irradiated samples was evaluated by extracting with N-N-dimethylacetamide at 80°C, for 50 hrs and dried in vacuum at about 50°C. The w_g was evaluated to be 0.58 and 0.66 for the 10 and 20 Mrads irradiated samples, respectively. In this work the irradiated crude samples were used without extracting their soluble fraction.

Deformation

The unirradiated and irradiated (uncrosslinked and crosslinked) samples were uniaxially stretched or compressed in two modes described below.

a) Elastic deformation; A piece of crosslinked samples (10 Mrad) was uniaxially stretched at a rate of 500 %/sec after melted perfectly in a silicon oil bath at 180°C to different extents and cooled to room temperature while holding the stretched length. For uniaxial compression, the 20 Mrad irradiated sample was compressed in the melt at 180°C between two metal plates and cooled to room temperature over a period of 15 min.

b) Plastic deformation; A piece of uncrosslinked samples was uniaxially stretched at a rate of 200 %/min at 100°C to different extents and after kept for 5 min it was cooled to room temperature. For uniaxial compression, the sample was compressed at a temperature of 150°C below the melting point between two metal plates. Biaxially stretching was also made for this sample. It was simultaneously stretched in two directions at a rate of 200 %/min at 150°C to different extents and after kept for 5 min it was cooled to room temperature.

In the procedures a) and b), the uniaxial or biaxial stretching and compression

were achieved in either the molten state or partially crystallized state. The stretched samples will be designated by the temperature when stretched and the draw ratio which is defined to be the ratio of the stretched length to the original length. The degree of compression was expressed by the ratio between the film thicknesses before and after compression.

Measurements of Crystal Transformation (from the α-form to the β-form) by Wide Angle X-ray Diffraction

The transformation of the crystal forms from α to β with the various modes of deformation or deformed-crystallization described above was examined with an X-ray analysis using the (002)-diffraction of the α-form and the (001)-diffraction of the β-form. The degree of the transformation was defined to be

$$\Phi_w = \frac{I_{\beta(001)}}{I_{\alpha(002)} + I_{\beta(001)}} \times 100\ (\%)$$

Here, $I_{\alpha(002)}$ and $I_{\beta(001)}$ are the integrated X-ray diffractions from the (002) and (001) crystal planes of the α and β forms, respectively. These quantities were obtained by an X-ray analysis using the relation,

$$I_{hkl} = \int_\theta d\theta \int_0^{\pi/2} X(\phi, \theta) \sin\phi\, d\phi$$

Here, X is a quantity to express the distribution function of P^*_{hkl} (the normal to the each crystal plane) to the stretching direction, when P^*_{hkl} makes an angle of ϕ to the stretching direction. The value of X was obtained as an X-ray diffraction intensity when the stretching direction of sample made the angle ϕ to the inner bisector of the X-ray incident and diffractive beams (the inner bisector of an angle, connecting the X-ray counter, sample, and X-ray incident beam). The angle θ designates the Bragg's angle of the each crystal plane and the integration concerning θ was done in the whole θ range where the diffraction from the crystal plane appeared.

Small Angle X-ray Scattering (SAXS)

The SAXS patterns were obtained at room temperature with a point collimation Rigaku Denki small angle X-ray camera. Ni-filtered Cu-K_α radiation was used. These X-ray working were carried out under vacuum with 50kV, 80mA, and 0.3 mm primary beam diameter and a specimen to film distance of 300 mm. A small angle camera with a Kratky collimation (Cu-K_α, scintillation counter) was used to obtain quantitative characteristics of small angle scattering. The long period, $d = \lambda/2\,\mathrm{Sin}\theta$ (where λ is the Cu-K_α wavelength and 2θ the scattering angle of the primary beam) was found from the position of the maximum in the scattering curve after subtraction of the diffuse scattering.

Estimation of Planar Orientation by Wide Angle X-ray Diffraction

In order to examine the planar orientation of crystal planes for uniaxially com-

pressed samples, X-ray diffraction analysis was carried out with a flat camera and a diffraction scan technique with a Ni-filtered Cu-K_α beam. These techniques are the same as were previously used or compressed crosslinked polyethylene.[6,7]

Thermal Properties

The fusion curve was obtained by a differential scanning calorimetry with use of the Perkin Elmer DSC 1-B by a heating rate of 10°C/min. The dimensional change was measured with increasing temperature in air under a constant load. The applied load was 1 g/mm^2, and dimensional change was followed by a cathetometer. The temperature was increased at the rate of 1°C/min.

RESULTS AND DISCUSSION

Crystal Transformation

X-ray photographs of PVDF samples drawn at temperatures from 50 to 180°C are shown in Fig. 1. These patterns were obtained with X-ray beam, normal to sample film and vertical to the drawing direction. It can be seen that the diffraction pattern depends on the draw temperature. The sample drawn at 50°C is found in one crystalline form, referred to as β-form. The samples drawn at 160°C are found in a mixture of β-form and another crystalline form, designated α-form. On the other hand, for samples crystallized from the melt under uniaxial stretch, no β-form is recognized and they exhibit highly oriented α-form crystal.

Figure 2 shows meridional X-ray diffraction for samples drawn at various temperatures. At first sight it is evident that each sample has highly oriented crystalline form. For a sample drawn at 100°C, the β-(001) diffraction peak in the vicinity of $2\theta=35°$ is strong but the α-(002) diffraction peak at $2\theta\simeq 39°$ is extremely small. However, as the draw temperature is increased the intensity of the β-(001) diffraction decreases and that of the α-(002) diffraction increases. These facts indicate that the fraction of α-form increases with increasing draw temperature; the crystalline form in drawn PVDF films is markedly influenced by draw temperature.

In Figs. 3 and 4 the degree of crystal transformation Φ_w for drawn sample are plotted against draw temperature and draw ratio, respectively. As can be seen from the figures, the value of Φ_w drastically decreases with increasing draw temperature. For samples drawn at 160°C, the value of Φ_w drastically increases with increasing draw ratio. On the contrary for samples drawn at the molten state, it does not increase appreciably with increasing draw ratio but to lesser extents. Thus, it is confirmed that the transformation of crystalline form, $\alpha\rightarrow\beta$, becomes pronounced as the drawing temperature decreases and the degree of drawing increases.

These results indicate that the macroscopic deformation at a low draw temperature is carried out accompanying the $\alpha\rightarrow\beta$ transition, pulling out the helical form of molecules (α form) into a planar zigzag conformation (β-form). At high draw temperature the drawing is carried out without the $\alpha\rightarrow\beta$ transition in the first step and the transformation $\alpha\rightarrow\beta$ occurs only at higher degrees of deformation. It was found that the relative ratio of the two crystalline forms depends on the variation in draw temperature and draw ratio.

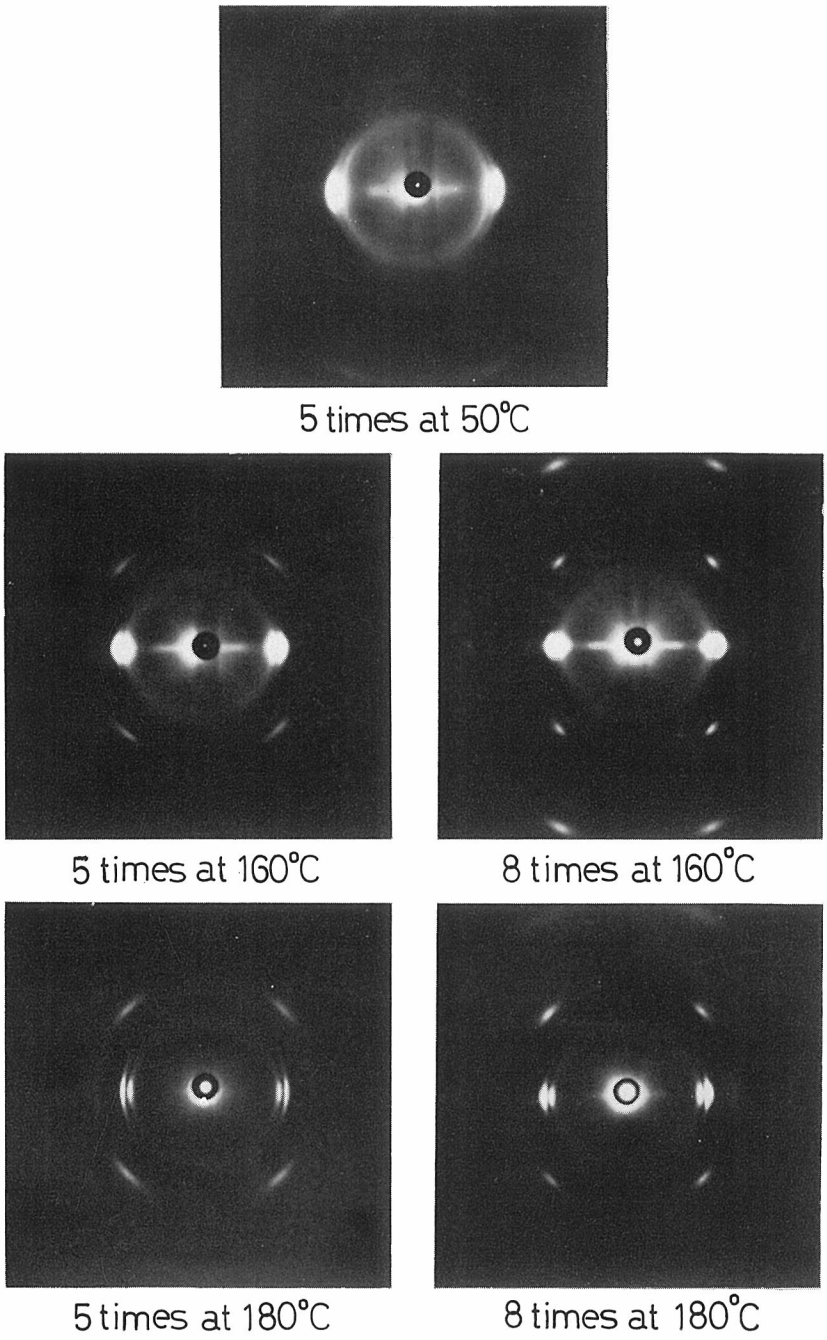

Fig. 1. Wide angle X-ray diffraction patterns of PVDF uniaxially stretched at various temperatures. X-ray beam was introduced perpendicular to the drawing direction (vertical in the figure).

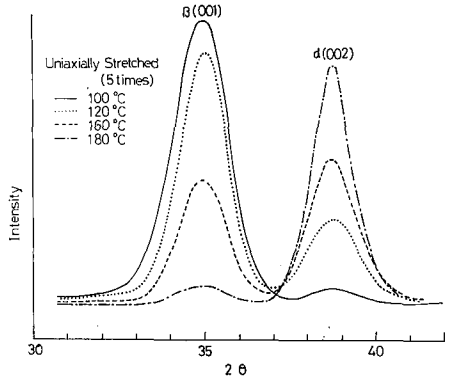

Fig. 2. Meridian scanning of X-ray diffraction for PVDF uniaxially stretched at various temperatures.

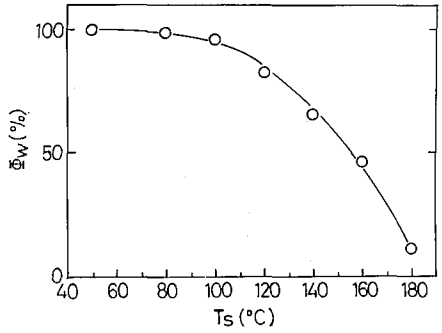

Fig. 3. Change in fraction of crystal transformation ($\alpha \rightarrow \beta$ form) with stretching temperature for PVDF 5 times uniaxially stretched at various temperatures.

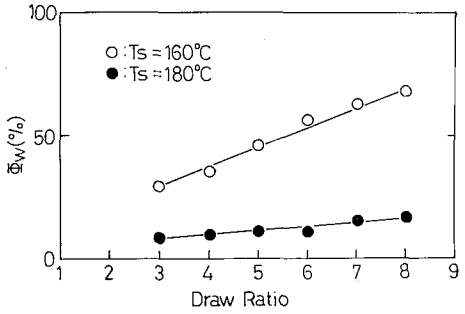

Fig. 4. Changes in fraction of crystal transformation ($\alpha \rightarrow \beta$ form) with drawing for PVDF uniaxially stretched at 160°C and at 180°C.

Small Angle X-ray Scattering

Next we consider the small angle X-ray scattering for samples drawn at 160°C and at the molten state to different degrees. Figure 5 shows the SAXS patterns for the two series of samples, stretched at 160°C in the partially crystalline state and at 180°C in the molten state, respectively. It is seen that, when stretched at 160°C, a diffuse six-point diffraction appears at a draw ratio of 2 and an arc-like shaped diffraction appears at a draw ratio of 3, and upon further drawing a discrete line diffraction appears, which shows an irregular lamella structure. On the other hand, when stretched at molten state the patterns obtained are quite different as can be seen from the figure. The two-point pattern is always recognized from the drawn sample independent of the draw ratio from 2 to 8-fold. The diffraction points approach the center of the pattern with increasing draw ratio, showing qualitatively increasing of the long period. Such two-point pattern has been reported for a stretched sample when it was shrunk with annealing at a high temperature (close to melting point)[18]. But we note here that the crosslinked sample drawn highly such as to 8-fold exhibits two-point shape without shrinkage.

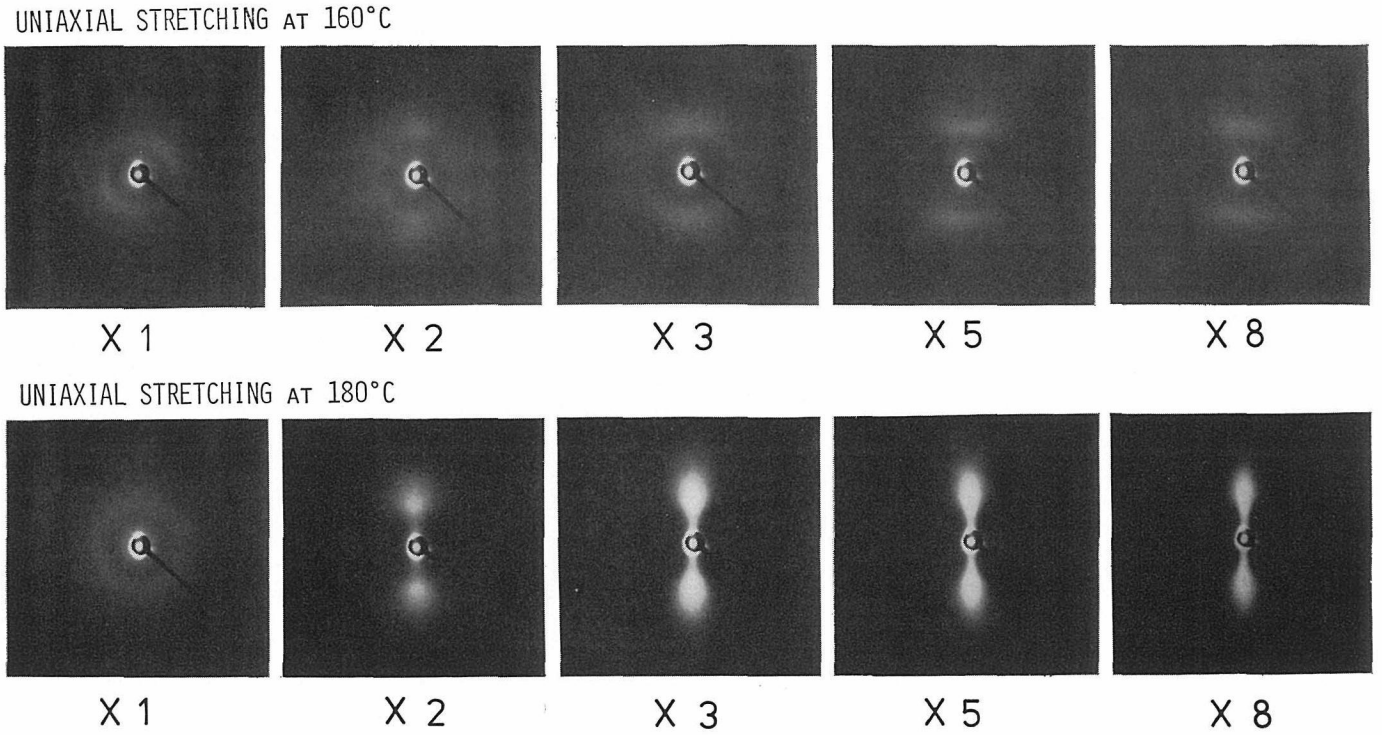

Fig. 5. Small angle X-ray diffraction patterns for PVDF uniaxially stretched to different degrees at 160°C (upper series) and at 180°C (lower series). X-ray beam was introduced perpendicular to the drawing direction (vertical in the figure).

The result implies that the drawing in the unmolten state produces enhanced disordering of the lamellar interfacial structure while the stretching in the melt does not produce such disordering.

In Figs. 6 and 7 the long period evaluated from the 2θ angle at the maximum and the maximum intensity are plotted against draw ratio for the two series of samples. When the uncrosslinked sample is stretched in the partially crystallized state,

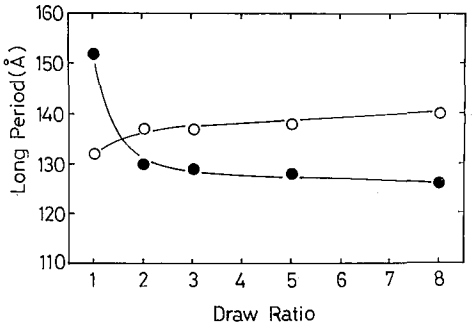

Fig. 6. Variation of the long period as a function of draw ratio for PVDF uniaxially stretched at 160°C (●) and at 180°C (○).

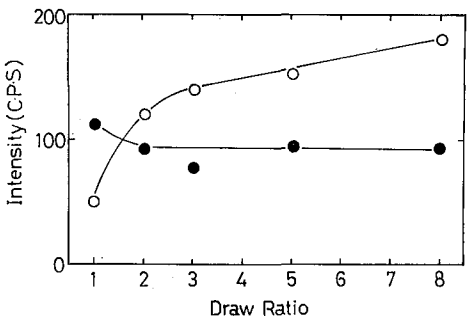

Fig. 7. Variation of the scattering intensity as a function of draw ratio for PVDF uniaxially stretched at 160°C (●) and at 180°C (○).

the long period decreases and the maximum intensity either decreases or stays unaltered as the draw ratio increases. This is similar to the case of the polyethylene and polypropylene samples, reported by Peterlin et al.[19,20] On the other hand, for the crosslinked sample drawn at molten state, the both of long period and maximum intensity evidently increase with increasing draw ratio. These phenomena were also recognized for the crosslinked polyethylene and polypropylene samples when they were crystallized from the melt under uniaxially stretched or compressed states.[11,13]

In any case the above-mentioned distinct difference in the small angle X-ray scattering phenomena between samples either crystallized from the melt under uniaxial stretching or stretched plastically in the partially crystalline state will be well reflected in the difference of the structure of both kinds of samples.

Orientation of Crystal Planes

X-ray diffraction photographs were obtained for samples prepared under different conditions. With an X-ray beam perpendicular to the film surface of sample, a Debye-Scherrer diffraction was obtained for all samples. This indicates random distribution of crystallites about the normal to the film surface. However, as can be seen in Fig. 8 with an X-ray beam parallel to the film surface, different types of X-ray patterns were obtained depending on the deformation condition. These patterns suggest that the planar orientation of some crystal planes exists in the samples to different degrees. As mentioned above, the transformation of the crystal forms $\alpha \rightarrow \beta$ takes place accompanying deformation. But here only planar orientation of the α-crystal form is considered since the melt-compressed samples

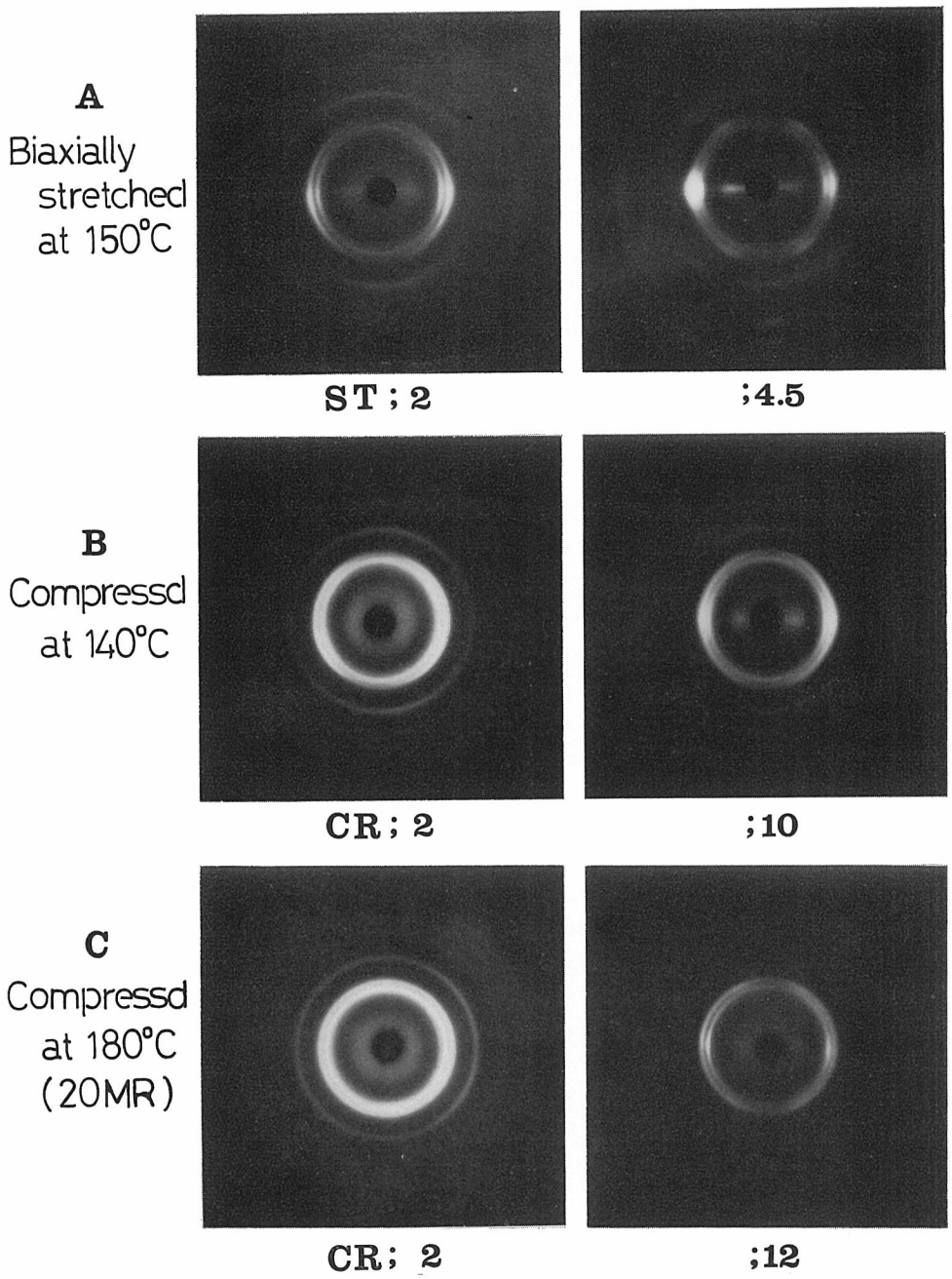

Fig. 8. Wide angle X-ray diffraction patterns for PVDF deformed under various conditions. X-ray beam was introduced parallel to the film surface.

are mostly in the α-form although the plastically deformed samples contain a β-crystal form.

The diffraction intensity $I(\phi)$ from each crystal plane (010), (200), (110) and (210) was recorded as function of the angle ϕ, by rotating the sample stepwise.

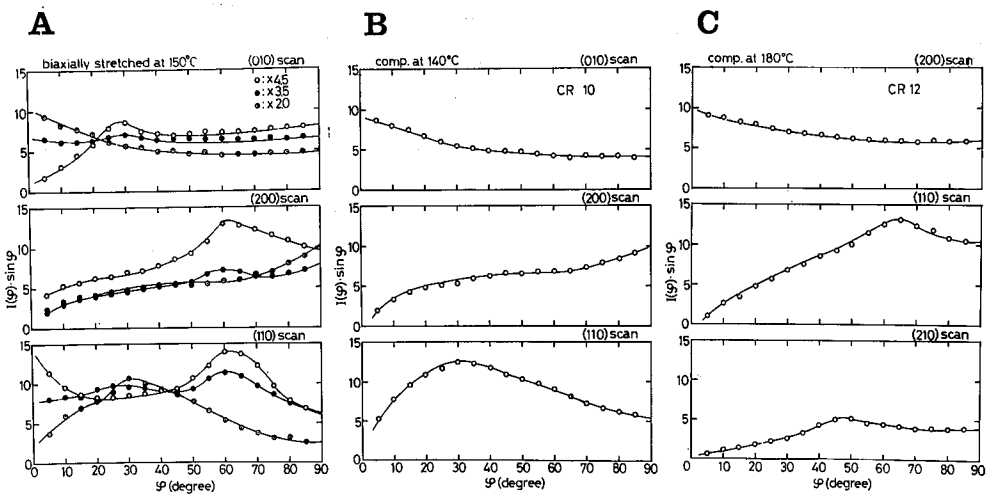

Fig. 9. I (ϕ) sin ϕ vs. ϕ of the crystal planes (010), (200), (110), and (210) for PVDF deformed at various conditions.

The detailed procedure and base line correction for the scan are described in previous papers.[6,7] The products $I(\phi)\sin\phi$ for the (010)-, (200)-, (110)-, and (210)-diffractions for the samples with different degrees of deformation are plotted against ϕ in Fig. 9. This product indicates the probability density that the vector P^* for each crystal plane points to the direction between ϕ and $\phi+d\phi$ in an arbitrarily chosen crystallite in samples. Hence, one can inquire the appearance of the crystal plane orientations with increasing degree of deformation by examining these figures. For samples biaxially stretched at 150°C [Fig. 9(A)] the value of $I\cdot\sin\phi$ for the (010) crystal plane has maximum at $\phi=0°$ for a draw ratio of 2, but as the draw ratio increases a peak in the vicinity of $\phi=28°$ appears. In the (200)-scan, $I\cdot\sin\phi$ has a maximum at $\phi=90°$ for a draw ratio of 2, but as the draw ratio increases a peak at about $\phi=63°$ appears. Similarly, in the (110)-scan, $I\cdot\sin\phi$ has a maximum at about $\phi=28°$ for a draw ratio of 2, but as the draw ratio increases a peak at $\phi=0°$ and about $\phi=56°$ appears. For the sample compressed at 140°C [Fig. 9(B)] the result is quite different; any planar orientation of crystal plane is not definitely recognized at a relatively low degree of compression. In the (010), (200), and (110) scans for a sample with compression ratio of 12, $I\cdot\sin\phi$ has maxima at $\phi=0°$, $\phi=90°$, and $\phi=28°$, respectively. For samples compressed to a compression ratio of 12 in the molten state of 180°C [Fig. 9(C)] $I\cdot\sin\phi$ has maxima at $\phi=0°$, $\phi=62°$, and $\phi=44°$ in the (200), (110), and (210) scans, respectively.

The results mentioned above should indicate the appearance of planar orientations of some crystal planes. We next consider these results referring to the reciprocal lattice diagram of the orthorhombic crystal form (α) shown in Fig. 10. The planar orientation of a crystal plane should be confirmed by the maxima or an increased value of $I\cdot\sin\phi$ at $\phi=0°$ in the respective scanning if it is assumed that the chain axes (c-axes) are parallel to the film surface. Hence, maximum or en-

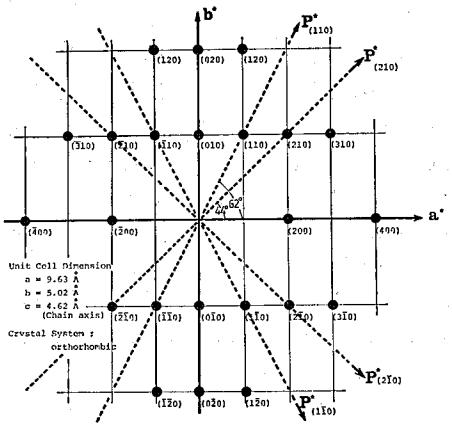

Fig. 10. a*- b* plot of the reciprocal lattice of the orthorhombic crystal form of PVDF. Here, c-axis (=c*-axis, molecular axis) is perpendicular to the a*- b* plane.

hanced values of $I \cdot \sin\phi$ at 0° for the (010) and (110) of the biaxially stretched sample (4.5×4.5) should indicate the planar orientation of these crystal planes. Since the vector P^*_{010} makes angles of 28° and 46° to vectors P^*_{110} and P^*_{120}, respectively, the maximum values of $I \cdot \sin\phi$ at ϕ=28° in the (110) scan and at 90° in the (200) scan are to be understood as additional evidence of the appearance of the (010) orientation. Similarly the (110) orientation will also be further certified by an increased value of $I \cdot \sin\phi$ at ϕ=28° in the (010) scan because P^*_{110} makes an angle of 28° with P^*_{010}. A minor (200) planar orientation can be detected by the increased value of $I \cdot \sin\phi$ at ϕ=0 for the sample compressed at 180°C in the (200) scan (Fig. 9(C)).

In Table II summarized the results of the planar orientation. When the crosslinked sample was crystallized from the melt under uniaxial compression, the (200) crystal plane is selectively oriented parallel to the film surface. On the other hand, for the sample deformed at a high temperature but below its melting point, it is confirmed that the (010) crystal plane is preferentially oriented parallel to the film surface at relatively low degrees of deformation, and the (110) crystal plane is oriented parallel to the film surface at higher degrees of deformation.

Table II. Planar Orientation of PVDF Films Obtained by Various Methods of Deformation

Simultaneously biaxial stretched at 150°C		Compressed at 140°C		Compressed at 180°C	
S.R*	Planar orientation	C.R*	Planar orientation	C.R*	Planar orientation
2	010_s**	4	010_w**	8	200_w**
3.5	010_w+110_w	6	010_w	10	200_s
4.5	110_s	10	010_s	12	200_s

* S.R=Stretch ratio
C.R=Compression ratio

** S=Strong
W=Weak

Thermal Properties

The DSC thermograms for samples drawn 4-fold at various temperatures are shown in Fig. 11. As the draw temperature is increased, the melting temperature increases. The fusion curve depends greatly on the preparation condition of samples. For the samples drawn at a temperature below melting point a small shoulder is observed in the low temperature range. However, for the sample drawn in the molten state an endothermic peak with a long "tail" persisting to 171°C is recognized. Similar persisting tail is sometimes reported for other polymers such as polyethylene,[6,9,11] polypropylene,[13] and polyvinyl alcohol[14] with abnormally high melting temperature, when the polymers are crystallized under conditions involving molecular orientation.

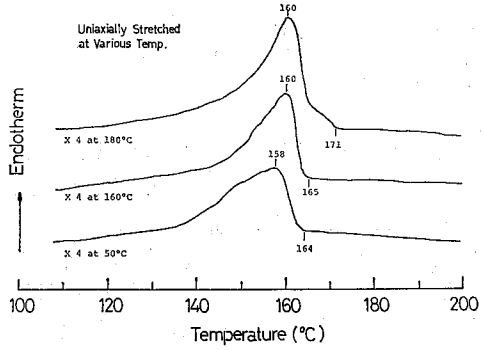

Fig. 11. DSC fusion curve for PVDF 4-fold uniaxially stretched at various temperatures.

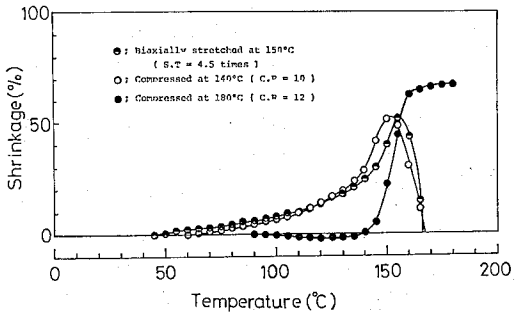

Fig. 12. Thermal shrinkage of PVDF films.

Figure 12 shows thermal shrinkage curves for the films deformed at temperatures below or above the melting point. The most remarkable feature is the difference between the samples compressed at temperature below the melting point and the sample compressed at the molten state. The former samples begin to shrink at about 50°C and the shrinkage increases continuously up to about the melting point, but the latter sample does not shrink up to 140°C at which a partial fusion of oriented crystallites may begin, and after going through this temperature it shrinks very rapidly. These shrinkage curves are quite similar to the curves for polyethylene[8] and polypropylene[13] made in a similar manner. The good dimensional stability of the melt-compression sample must be caused by its relaxed amorphous chains and the perfection of the crystalline phase in the structure.

CONCLUSION

The crosslinked polyvinylidene fluoride, when highly stretched or compressed in the molten state, exhibits a unique phase structure with characteristic thermodynamic and physical properties similar to other polymers such as crosslinked polyethylene and polypropylene. The sample stretched uniaxially in the molten state is characterized by a very ordered crystalline phase and rather unoriented and relaxed

amorphous material. The orientation factor to the stretching direction for the chain axes in the crystalline phase is very close to unity but that in the amorphous phase stays in a low level.

When compressed uniaxially in the molten state, a special planar orientation of the crystal planes of the orthorhombic form of this polymer appears in which the (200) crystal plane is preferentially oriented parallel to the film surface while no appreciable amount of the β-form appears. On the contrary, when compressed or biaxially stretched in the partially crystallized state, other planar orientations such as the (010) and (110) planar orientations are produced without the (200) orientation. This result indicates that this mode of crystallization involves less restriction to the molecular mobility during the crystallization despite of the high degrees of compression.

REFERENCES

(1) Ye.L. Gal'perin, B.P. Kosmynin, L.A. Aslanyan, N.P. Mlenik, and V.K. Smirnov, *Vysokomol. Soyed.*, **A12**, 7 (1970).
(2) W.W. Doll and J.B. Lando, *J. Macromol. Sci. Phys.*, **B4**, 889 (1970).
(3) J.B. Lando, H.G. Olf, and A. Peterlin, *J. Polymer Sci.*, **A-1, 4** 941 (1966).
(4) Ye.L. Gal'perin, Yu.V. Strogalin, and M.P. Mlenik, *Vysokomol. Soyed.*, **7**, 933 (1965).
(5) B.P. Kosmynin, Ye.L. Gal'perin, and D.Ya. Tsvankin, *Vysokomol. Soyed.*, **A12**, 1254 (1970).
(6) R. Kitamaru, H.-D, Chu, and S.-H. Hyon, *Macromolecules*, **6**, 337 (1973).
(7) S.-H. Hyon, H. Taniuchi, and R. Kitamaru, *Bull. Inst. Chem. Res., Kyoto Univ.*, **51**, 91 (1973).
(8) R. Kitamaru, C. Tsuchiya, and S.-H. Hyon, *ibid.*, **52**, 436 (1974).
(9) R. Kitamaru and S.-H. Hyon, *Makromol. Chem.*, **175**, 255 (1974).
(10) S.-H. Hyon, R. Kitamaru, H. Taniuchi, N. Hayakawa, and N. Tamura, *Kobunshi Ronbunshu*, **32**, 240 (1975).
(11) R. Kitamaru and S.-H. Hyon, *Macromolecular Review*, **14**, 203 (1979).
(12) R. Kitamaru and S.-H. Hyon, *J. Polym. Sci. Polym. Phys.*, **13**, 1085 (1975).
(13) S.-H. Hyon and R. Kitamaru, *J. Appl. Polym. Sci.*, to be published
(14) S.-H. Hyon, H.-D. Chu, and R. Kitamaru, *Bull. Inst. Chem. Res., Kyoto Univ.*, **53**, 367 (1975).
(15) C.W. Wilson and E.R. Santee, *J. Polym. Sci.*, **C3**, 97 (1965).
(16) G.J. Melch, *Polymer*, **15**, 429 (1974).
(17) R. Timmerman, *J. Appl. Polym. Sci.*, **22**, 456 (1962).
(18) B.P. Kosmynin, Ye.L. Galperin, and D. Ya Tsvankin, *Vysokomol. Soyed.*, **A14**, 1365 (1972).
(19) A. Peterlin and R. Cornelliussen, *J. Polym. Sci.*, **A-2, 6**, 1273 (1968).
(20) F.J. Balta-Calleja and A. Peterlin, *J. Materials Sci.*, **4**, 722 (1969).